Preparation of High-Performance Damping Materials Based on Carboxylated Nitrile Rubber: Combination of Organic Hybridization and Fiber Reinforcement

Qi-Xia Liu, Xin-Bo Ding, Hui-Ping Zhang, Xiong Yan

Key Laboratory of Textile Science and Technology, Ministry of Education, College of Textiles, Donghua University, Shanghai 201620, China

Received 27 March 2008; accepted 4 January 2009
DOI 10.1002/app.29997
Published online 8 July 2009 in Wiley InterScience (www.interscience.wiley.com).

ABSTRACT: The dynamic mechanical properties denoted by storage modulus (E') and loss factor (tan δ) of binary and ternary systems consisting of carboxylated nitrile rubber (XNBR) filled with organic hindered phenol compound 2,2′-methylenebis(6-*tert*-butyl-4-methylphenol) (AO-2246) or/and short carbon fiber (SCF) were investigated. DMA results of binary XNBR/AO-2246 system showed that by addition of AO-2246, the tan δ peak maximum of XNBR was remarkably increased up to 3.5, and its peak position was also significantly shifted to room temperature, demonstrating that XNBR/AO-2246 composite is a promising damping material. Nevertheless, application of such XNBR/AO-2246 composite is limited due to its relatively low E' value above glass transition temperature. Therefore, to develop a high-performance damping material with high tan δ peak and high modulus as well as controllable tan δ peak position, the combination of organic hybridization and fiber reinforcement were adopted. DMA analysis of various ternary XNBR/AO-2246/SCF systems revealed that by introduction of SCF, the E' value of XNBR/AO-2246 was increased remarkably while the tan δ peak maximum was still higher than 2.5. Thus, a new type of XNBR-based high-performance damping material was developed. © 2009 Wiley Periodicals, Inc. J Appl Polym Sci 114: 2655–2661, 2009

Key words: carboxylated nitrile rubber (XNBR); damping material; organic hybridization; fiber reinforcement; dynamic mechanical analysis

INTRODUCTION

Polymers are typical candidate damping materials for their unique viscoelastic properties. Their damping properties are dominated by the glass transition. When a polymer is heated from a glassy state, the chain segments in its backbone begin to make the Gennes-like reptation motion. The mechanical energy of the molecular vibrational motion is converted into heat energy, and a loss peak appears in the glass transition temperature (T_g) range.[1] Thus, polymers with higher damping peaks around the application temperature are preferred. However, most polymers are not satisfying due to their distant T_gs from the application temperature or relatively lower damping peaks. Moreover, their relatively low modulus at higher temperature often limits their engineering applications to some extent. Hence, much research has been done on damping modification of polymeric materials in an attempt to obtain high-performance damping materials with high damping peak, high modulus, as well as controllable damping peak position to meet different practical requirements.

In general, the height and position of the damping peak of a given homopolymer at a given frequency can be changed within a certain range by many conventional means, such as the addition of plasticizers and fillers. However, the addition of plasticizers can indeed lead to an increase in the damping peak height, but the damping peak position is often shifted to a lower temperature and the storage modulus is also reduced.[2,3] On the other hand, the introduction of inorganic particles or fibers can provide high strength and modulus, whereas the damping peak height is decreased sharply while the damping peak position is slightly shifted.[4,5] These facts show that the improvement of damping peak height and modulus as well as the control of damping peak position cannot be accomplished simultaneously by conventional means. Recently, a kind of novel organic hybrid damping material consisting of a polar polymer such as chlorinated polyethylene (CPE), chlorinated polypropylene (CPP), and acrylate rubber (ACM) and some functional organic small molecular substances have drawn much attention.[6–13] Results show that the addition of a large amount of hindered amine or hindered phenol compounds

Correspondence to: X. Yan (yaxi@dhu.edu.cn).

such as *N,N′*-dicyclohexyl-benzothiazyl-2-sulfenamide (DZ) and 3,9-bis[1,1-dimethyl-2{β-(3-*tert*-butyl-4-hydroxy-5-methylphenyl)propionyloxy}ethyl]-2,4,8,10-tetraoxaspiro[5,5]-undecane (AO-80) can greatly improve the damping peak height of CPE, CPP, and ACM due to the organic hybridization effect caused by the formation of a reversible hydrogen bonding interaction between matrix polymers and organic small molecular substances. The damping peak position also can be adjusted by changing the content of small molecular substances. This will provide a new design concept for developing good damping materials based on the sophisticated use of hydrogen bonds, though the reduced storage modulus above T_g of such organic hybrids needs to be improved further.

For such organic hybrid damping systems, the selection of matrix polymers and organic low molecular substances is of vital importance. Compatibility between the two components has a great influence on the dynamic mechanical properties of organic hybrid systems.[14] Polar polymers such as CPE, CPP, and ACM are commonly used matrix polymers. Chlorinated butyl rubber (CIIR), nitrile butadiene rubber (NBR), as well as epoxidized natural rubber (ENR) have recently been reported as matrix polymers in organic hybrid systems.[15–17] Carboxylated nitrile rubber (XNBR) is a kind of modified NBR with carboxyl group.[18,19] Compared with NBR, XNBR has larger polarity, which leads to good compatibility with polar or nonpolar resins and a higher degree of interaction with fillers as well as enhanced physical and mechanical properties, oil resistance, and processability. Moreover, its damping property is greatly improved with a loss factor (tan δ) of 1.8, showing a great potential for damping material. Therefore, in this paper, based on the new design concept of organic hybrids, XNBR was chosen as the matrix polymer, and organic hindered phenol compound 2,2′-methylene-bis(6-*tert*-butyl-4-methylphenol) (AO-2246) with two hydroxyl groups was added to obtain a new organic hybrid system with high damping property. Furthermore, a kind of commonly used reinforcement filler for polymers, short carbon fiber (SCF) with high strength and modulus, was incorporated into the binary XNBR/AO-2246 system to improve its storage modulus. The purpose of this paper was to prepare a new type of XNBR-based high-performance damping material with a high damping peak and high modulus as well as controllable damping peak position by combination of organic hybridization and fiber reinforcement. The dynamic mechanical properties of various binary XNBR/AO-2246 systems and ternary XNBR/AO-2246/SCF systems were investigated by dynamic mechanical analysis (DMA).

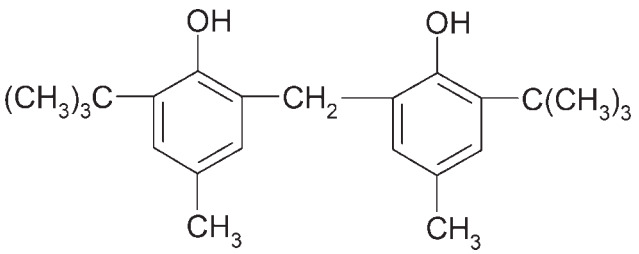

Figure 1 Chemical structure of AO-2246.

EXPERIMENTAL

Materials

The XNBR used as matrix in this study, with an acrylonitrile degree of 40 wt % and a carboxyl degree of 3 wt %, is rubbery grade (manufactured by Nanjing Shengdong Chemical, Nanjing, China). The SCF used as reinforcement filler has a density of 1.8 g/mm^3 and a diameter of 7.8 μm and an average length of 2.0 mm (manufactured by Toho Chemical Industry, Tokyo, Japan). The organic low molecular weight hindered phenol compound (AO-2246), as shown in Figure 1, is a commercially available antioxidant (supplied by Nanjing Hua Lim, Nanjing, China).

Sample preparation

XNBR powders were first kneaded for 5 min at ca. 60°C on a two-roll mixing mill (SK-160B). Different weight fractions of AO-2246 or/and SCF were incorporated into the kneaded XNBR and blended further for another 15–30 min, depending on different filler loading. No other rubber additives such as plasticizer, vulcanizing agent, or cross-linking agent were used. The mixtures were made molten for 5 min and then compression-molded for 10 min at 140°C under a pressure of 10 MPa, using a small laboratory press (QLB-D350×350×2). Finally, the molded samples were taken out and cooled by icewater quenching to obtain sheets with a thickness of about 1 mm.

Measurements

Dynamic mechanical analysis

Dynamic mechanical analysis (DMA) measurements were carried out using a dynamic mechanical analyzer (DMA-7, Perkin Elmer) in a tension mode at a constant frequency of 1 Hz and a varied temperature from −50 to 100°C with a heating rate of 5°C/min. During the measurement the strain amplitude was held fixed, and both the static and the dynamic forces were adjusted. The ratio of static force to dynamic force amplitude was held fixed at a value of 110% to prevent the sample from being torn apart when the viscosity decreased above the glass

transition. The parallelepiped specimens were 12 mm long, 4 mm wide, and around 1 mm thick.

Differential scanning calorimetry

Differential scanning calorimetry (DSC) measurements were carried out with a Pyris-1 Perkin Elmer calorimeter. Samples about 5 mg in weight and sealed in aluminum pans were heated from 40 to 200°C at a heating rate of 20°C/min under a high purity helium atmosphere with a gas flow rate of 20 mL/min.

Scanning electron microscopy

Scanning electron microscopy (SEM) observation was performed with a JEOL JSM-5600LV apparatus. Prior to SEM observations, liquid nitrogen–fractured surfaces of the composites were gold sputtered.

RESULTS AND DISCUSSION

Binary XNBR/AO-2246 system

Figure 2 shows the temperature dependence of the loss factor (tan δ) for various XNBR/AO-2246 samples. As shown in the figure, all the XNBR/AO-2246 blends show a single tan δ peak associated with T_g of XNBR, and the tan δ peak height increases and its peak position shifts toward higher temperatures as the AO-2246 content increases. The growth and peak shift of tan δ peak in the XNBR/AO-2246 blends demonstrate that AO-2246 is compatible with XNBR. Moreover, it is noted that with increasing the AO-2246 content, the tan δ peak height increases up to 50 wt % of AO-2246 and then becomes smaller. This suggests that when the AO-2246 content is larger than a critical value, a kind of new phase morphology may be formed in the XNBR/AO-2246 system.

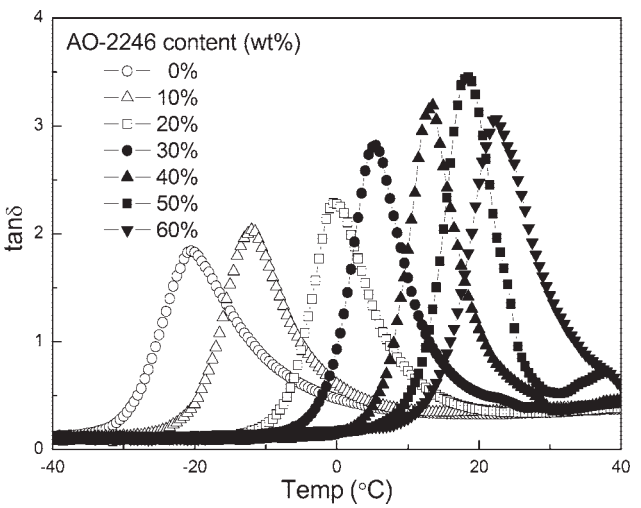

Figure 2 Temperature dependence of tan δ at 1 Hz for various XNBR/AO-2246 samples.

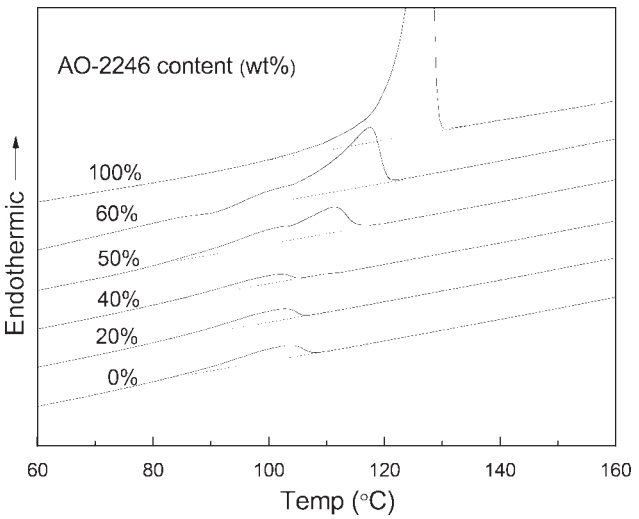

Figure 3 DSC melting endotherms of various XNBR/AO-2246 samples.

To investigate the dispersion state of AO-2246 molecules in the matrix polymer XNBR, DSC measurement was performed. Figure 3 shows the DSC curves of XNBR, AO-2246, and XNBR/AO-2246 samples. As seen in the figure, the pure XNBR is only slightly crystallized and the pure AO-2246 is highly crystallized with a melting point (T_m) of 127°C. For the XNBR/AO-2246 sample, which was melt-pressed above the T_m of AO-2246 and thereafter cooled by quenching in icewater, the melting peak of AO-2246 vanished, whereas the melting peak of XNBR due to the residual crystallization of some other small molecules added during the process of manufacturing XNBR is only slightly decreased. The disappearance of the melting peak of AO-2246 suggests that AO-2246 molecules existed in an amorphous form or very finely dispersed in XNBR. This is because during hot-pressing at 140°C, AO-2246 particles melted into liquid form and thus dissolved more easily into the XNBR matrix. Consequently, during dispersing, the AO-2246 molecules were more likely to form strong interaction with the polar groups in the XNBR matrix. The formation of intermolecular hydrogen bond between XNBR and AO-2246 were confirmed through FTIR measurements, as shown in Figure 4. For XNBR/AO-2246, there are three main absorption regions in the infrared spectra that are sensitive to the hydrogen-bond formation, including the hydroxyl group (OH) stretching region locates within 3000–3600 cm^{-1}, the nitrile group (C≡N) stretching region within 2200–2300 cm^{-1}, as well as the carbonyl group (C=O) stretching region within 1700–1850 cm^{-1}. The C≡N and C=O of XNBR yield two absorption bands centering at 2237 cm^{-1} and 1725 cm^{-1}, respectively, whereas AO-2246

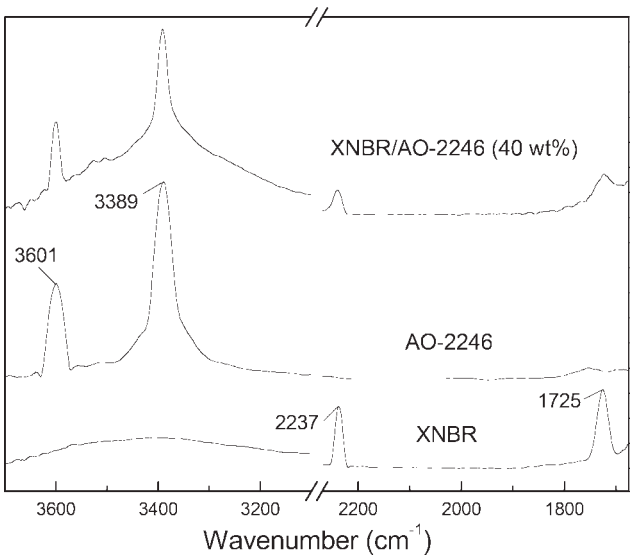

Figure 4 Infrared spectra of XNBR, AO-2246, and XNBR/AO-2246 (40 wt %) sample in the OH stretching region and the C≡N and C=O stretching regions.

shows no absorption in these regions. Therefore, any changes observed in these regions should be directly attributed to changes of the chemical environment of C≡N and C=O of XNBR, such as the formation of hydrogen bonds.[20] As seen in Figure 4, in the spectra of XNBR/AO-2246 (40 wt %), the two bands corresponding to C≡N and C=O of XNBR both decrease remarkably and become wider, especially for the C=O band. This suggests that by addition of AO-2246, the number of free C≡N and C=O of XNBR decreased, which may be caused by the formation of intermolecular hydrogen bond with OH of AO-2246 molecules.

It can also be seen from Figure 4 that the salient feature of the spectrum of pure AO-2246 is the presence of two significant absorption bands in the OH stretching region. The band at 3601 cm^{-1} is assigned to free (nonhydrogen-bonded) OH, whereas the band at 3389 cm^{-1} should be assigned to self-associated (OH—OH hydrogen-bonded) OH of AO-2246 molecules, due to its position with low wavenumber. For pure XNBR, only a very weak broad band centered at 3412 cm^{-1} is observed in this region, which should be attributed to the stretching vibration of the chain-end OH of XNBR. Because of the very low intensity of this band compared with that of AO-2246 in this region, its contribution to the total spectrum can be neglected when the content of AO-2246 is high enough. For XNBR/AO-2246 (40 wt %), the two bands corresponding to OH stretching vibration of AO-2246 both decrease sharply while a new large broad band appears. This new large broad band may be attributed to the superposition of the absorption band corresponding to the OH—C≡N intermolecular hydrogen bond between C≡N of XNBR and OH of AO-2246 and that corresponding to the OH—C=O intermolecular hydrogen bond between C=O of XNBR and OH of AO-2246. The large intensity of this broad band suggests the formation of a large amount of intermolecular hydrogen bonds in the XNBR/AO-2246 (40 wt %) sample, which in turn hindered the crystallization of AO-2246 molecules and led to the hybridization of XNBR and AO-2246 molecules, as is evident from the disappearance of the melting peak of AO-2246. However, it is seen in Figure 3 that the melting peak of AO-2246 in the XNBR/AO-2246 hybrids appears again when AO-2246 content is more than 40 wt % and the peak intensity increases with increasing AO-2246 content. These results demonstrate that a critical AO-2246 content of 40 wt % exists for XNBR/AO-2246 hybrids. When the AO-2246 content is smaller than this critical value, XNBR and AO-2246 are compatible, but when the AO-2246 content is higher than this critical value, a phase separation between XNBR and AO-2246 occurs, and when more AO-2246 is added, the excess AO-2246 molecules are crystallized in the AO-2246 domain. The change of phase morphology in XNBR/AO-2246 hybrids was further confirmed by SEM observation.

Figure 5 shows the SEM images of various XNBR/AO-2246 samples. In the XNBR/AO-2246 (40 wt %) system, all the XNBR and AO-2246 molecules are hybridized and the system demonstrates a special flower-like morphological structure. However, in the XNBR/AO-2246 (50 wt %) system with the AO-2246 content larger than the critical value, a part of excess AO-2246 molecules begins to aggregate and thus a microseparated morphology forms. With further increasing AO-2246 content, more excess AO-2246 molecules show self-aggregation and are crystallized in the reorganized AO-2246 domains; thus the intensity of the melting peak of AO-2246 increases. Such change of the phase morphology finally led to the change of viscoelastic properties of the XNBR/AO-2246 hybrids.

Figure 6 shows the AO-2246 content dependence of tan δ peak maximum (tan δ_{max}) and tan δ peak position (T_g) for various XNBR/AO-2246 hybrids. As shown in the figure, the tan δ_{max} value increases remarkably and its position shifts toward higher temperature with the increase of AO-2246 content due to the organic hybridization effect, which can be attributed to the formation of a large amount of strong intermolecular hydrogen bond between XNBR and AO-2246 as interpreted above. Besides, it can be noted that a turning point exists on the tan δ_{max} curve at certain AO-2246 content. However, it is interesting that the AO-2246 content of 50 wt % at the turning point is larger than the critical value observed from DSC curves. When AO-2246 content is lower than 40 wt %, all AO-2246 molecules are

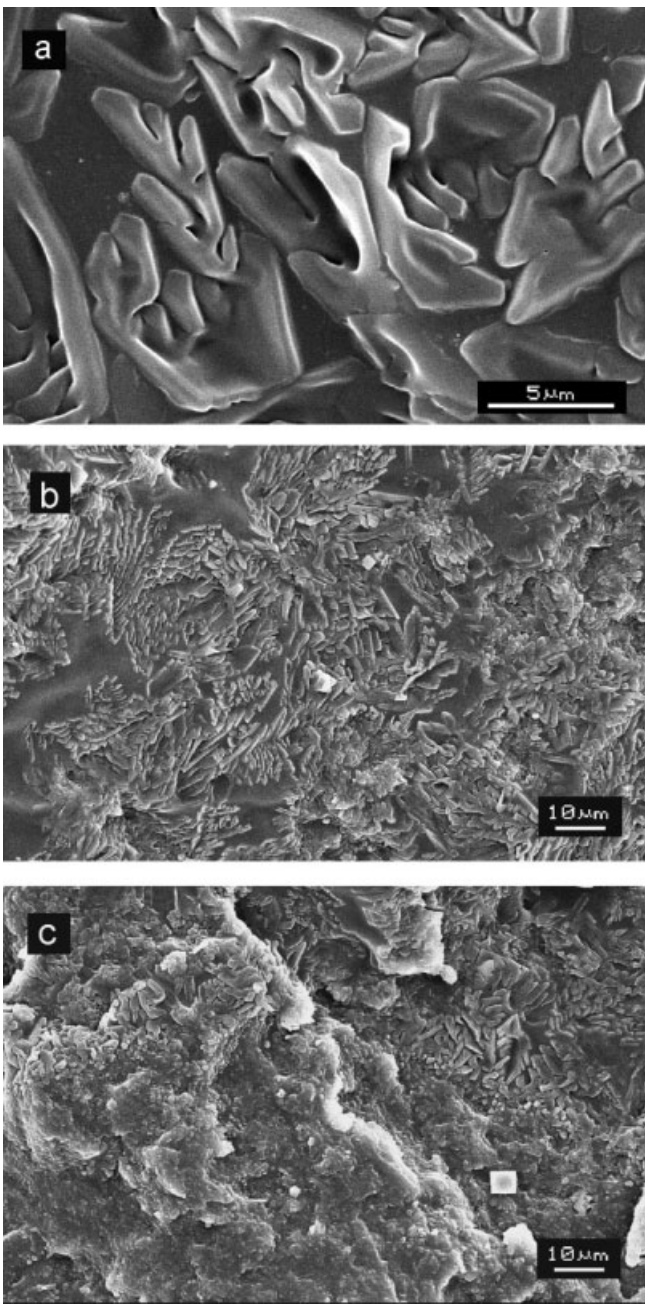

Figure 5 SEM images of various samples: (a) XNBR/AO-2246 (40 wt %); (b) XNBR/AO-2246 (50 wt %); (c) XNBR/AO-2246 (60 wt %).

hybridized with XNBR and the AO-2246 molecules are finely dispersed in an amorphous form. The hybridization of XNBR and AO-2246 leads to a significant increase of the tan δ peak height. With further increasing AO-2246 content up to 50 wt %, the tan δ value increases more sharply due to the contribution of an aggregate of a part of the microphase-separated AO-2246 molecules in addition to the hybridization effect.[7] However, the tan δ value begins to decrease above 50 wt % content of AO-2246 because more and more AO-2246 aggregates form into crystalline particles that can lower the tan δ peak. In this case, the positive impact of hybridization and the negative impact of crystallization on the tan δ value coexisted while the latter predominated over the former; thus the tan δ value decreased.

In summary, it can be concluded from the results above that addition of AO-2246 into XNBR leads not only to a remarkable increase in the tan δ peak maximum but also a significant shift of its position to room temperature, showing that XNBR/AO-2246 composite is a promising damping material.

Nevertheless, it is reported that by the addition of AO-80 into CPE or ACM, the storage modulus increases below the glass transition temperature but decreases above the glass transition temperature. The E' of CPE/AO-80 or ACM/AO-80 hybrids in higher temperature regions above T_g is smaller than that of pure CPE and even decreases with increasing AO-80 content.[6,9,21] Similar results were observed in XNBR/AO-2246 hybrids. As a result, applications of such organic hybrid damping material hybrids are limited to some extent due to their relatively low storage modulus above the glass transition temperature. To develop a high-performance damping material with both good damping property and high modulus, some other means should be combined with organic hybridization.

Ternary XNBR/AO-2246/SCF system

In recent years, short fiber reinforced rubber composites (SFRC), which combine the flexibility of matrix and the strength and rigidity of fiber together, are being increasingly employed as engineering materials for their superior mechanical properties, design flexibility, and favorable cost. Since SFRC undergo various types of dynamic stress during practical

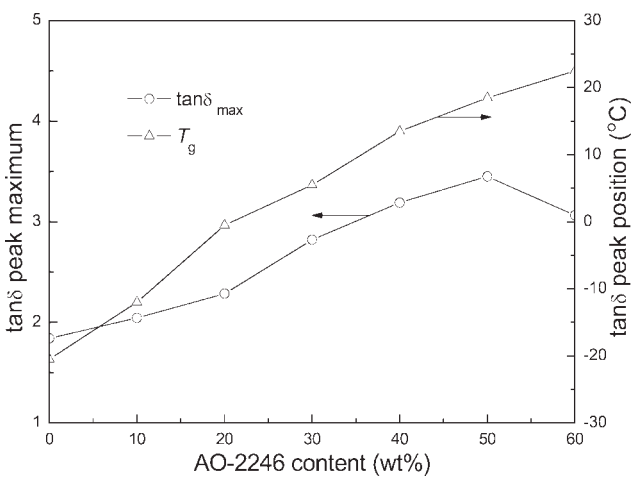

Figure 6 Dependence of tan δ peak maximum and its position for various XNBR/AO-2246 hybrids on the AO-2246 content.

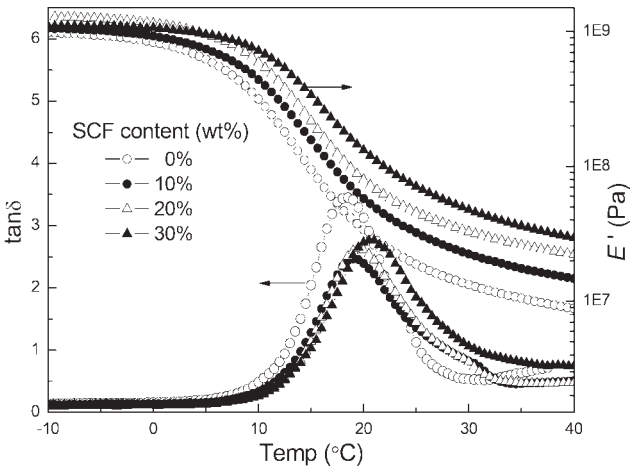

Figure 7 Temperature dependence of tan δ and E' at 1 Hz for XNBR/AO-2246 (1 : 1) with SCF.

application, studies on the dynamic mechanical properties of these materials are of great importance. Reports on dynamic mechanical properties of various SFRC show that by the incorporation of short fibers into the matrix, the storage modulus (E') and loss modulus (E'') were increased, whereas the mechanical loss factor (tan δ) was decreased, leading to a limited damping efficiency though the modulus is markedly improved. Thus, combination of organic hybridization and fiber reinforcement are adopted to develop a high-performance damping material with both good damping property and high modulus. A certain amount of short carbon fiber (SCF) with high strength and high modulus was added into the binary XNBR/AO-2246 (1 : 1) system. Figure 7 shows the temperature dependence of E' and tan δ for XNBR/AO-2246 (1 : 1) filled with 10, 20, and 30 wt % SCF. As shown in the figure, by introduction of SCF, the E' value of the binary XNBR/AO-2246 system is remarkably increased, especially in higher temperature regions above T_g, which shows the reinforcing effect of SCF fibers on the modulus. It is also clear from Figure 7 that the reinforcing effect becomes more obvious with increasing fiber content. This is mainly due to the increased contribution of the high modulus of SCF fiber itself toward the modulus of the composite with increasing fiber content. It can also be attributed to the increased interface area between fiber and matrix, which allows more efficient stress transfer from the matrix to the fibers.[22] The remarkably improved modulus provides better practical engineering value for the material.

It was also found that by introduction of SCF, the tan δ peak was lowered, as expected, due to the dilution effect, but the tan δ_{max} value was still greater than 2.5. Moreover, when SCF content exceeded 10 wt %, the tan δ peak maximum began to increase with increasing fiber content. This can be attributed to the increased friction between fibers at a higher fiber loading, which can also contribute to the damping characteristics of the ternary system.[5]

It can be drawn from the analysis above that by the introduction of SCF into binary XNBR/AO-2246 (1 : 1) system, the E' value is improved significantly while the tan δ_{max} value is maintained above 2.5, which is still much higher than that of most SFRC materials. Thus, a kind of high-performance damping material with better practical engineering value with both good damping property and high modulus is obtained by adding SCF fibers into XNBR/AO-2246 organic hybrids. However, it should be noted that the tan δ peak position of binary XNBR/AO-2246 system hardly changes with increasing of the SCF content due to the absence of strong interaction between fiber and matrix. The slight shift of the peak position toward higher temperatures (less than 3°C) is associated with the decreased mobility of the polymer chains by the introduction of fibers.[23] As interpreted in the first part, the tan δ peak position of the binary XNBR/AO-2246 system increases significantly with increasing AO-2246 content due to the strong hydrogen bonding interaction between XNBR and AO-2246. Therefore, the tan δ peak position of the ternary XNBR/AO-2246/SCF system can be supposed to be adjusted by fixing the weight ratio of XNBR/SCF while changing the AO-2246 content. Figure 8 shows the temperature dependence of tan δ for XNBR/SCF (9 : 1) filled with 10–50 wt % AO-2246. As shown in the figure, the XNBR/SCF (9 : 1) system exhibits a relatively low tan δ peak at a temperature much lower than room temperature. By the incorporation of AO-2246, the tan δ peak shifts significantly toward higher temperatures, as predicted, showing a controllable tan δ peak position

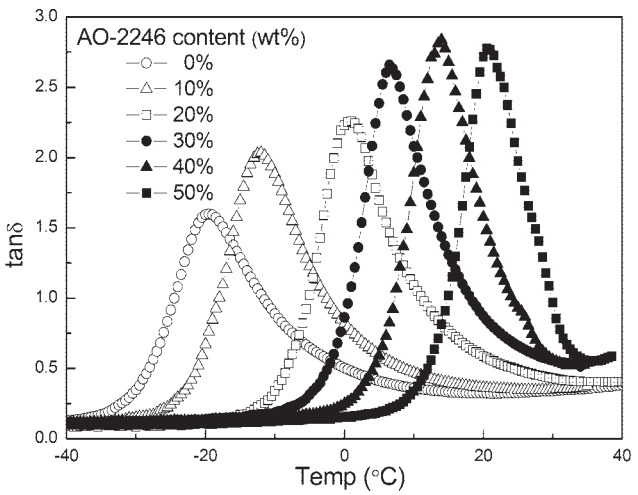

Figure 8 Temperature dependence of tan δ at 1 Hz for XNBR/SCF (9 : 1) with AO-2246.

for the ternary system. Meanwhile, the tan δ peak height increases remarkably up to 2.8 with increasing AO-2246 content. These results imply that ternary XNBR/SCF(9 : 1)/AO-2246 composites are high damping materials with controllable tan δ peak position. Furthermore, it is interesting that the tan δ peak height increases up to 40 wt % content of AO-2246 and then becomes lower above 40 wt % content of AO-2246, showing a turning point. The appearance of the turning point is attributed to the change of phase morphology when AO-2246 content is larger than a critical value as interpreted above. Compared with the binary XNBR/AO-2246 system in Figure 2, the AO-2246 content at the turning point of the ternary XNBR/SCF/AO-2246 system is smaller. This is because the presence of SCF fiber hindered the hybridization of XNBR and AO-2246 so that more AO-2246 molecules self-aggregated and formed into crystalline particles easily, which led to a negative impact on the tan δ_{max} value.

To sum up, combination of the organic hybridization effect of AO-2246 and the reinforcement effect of SCF on dynamic mechanical properties of XNBR obtains a new type of high-performance damping material possessing both good damping property and high modulus; at the same time, its damping peak position can be controlled by varying weight ratio of the components to meet different practical requirements.

CONCLUSIONS

Based on the new design concept of organic hybrid damping materials, a new organic hybrid XNBR/AO-2246 system was prepared. DMA results showed that addition of AO-2246 into XNBR led not only to a remarkable increase of the tan δ_{max} value up to 3.5 but also a shift of its peak position to room temperature as a result of the hybridization of the two components. Moreover, it was found that the change of phase morphology of XNBR/AO-2246 system at a higher AO-2246 content had a significant influence on the damping properties of the system and led to a turning point at the tan δ_{max}–AO-2246 content curve. Nevertheless, applications of XNBR/AO-2246 hybrids are limited to some extent due to their relatively low modulus at higher temperatures. Consequently, reinforcement filler SCF was introduced into binary XNBR/AO-2246 hybrids. Dynamic mechanical analysis of various ternary XNBR/AO-2246/SCF systems revealed that the modulus and damping property largely depended on the composition. A new type of XNBR/AO-2246/SCF high-performance damping materials with high modulus and high damping peak as well as controllable damping peak position to meet different practical requirements were thus obtained by changing the weight fraction of SCF or/and AO-2246 in the ternary systems. Thus, combination of organic hybridization and fiber reinforcement can be a new way of developing high-performance damping materials.

Another problem faced by organic hybrid damping materials in practical engineering application is ageing, which decreases the damping peak height of organic hybrids sharply during long-term service. Therefore, further efforts made to improve the damping stability for XNBR/AO-2246 organic hybrids during ageing or the heating process will be carried out in another article.

References

1. Mao, X. D.; Xu, S. A.; Wu, C. F. Polym Plast Technol Eng 2008, 47, 209.
2. Piorkowska, E.; Kulinski, Z.; Galeski, A.; Masirek, R. Polymer 2006, 47, 7178.
3. Liang, G. G.; Cook, W. D.; Sautereau, H. J.; Tcharkhtchi, A. Eur Polym J 2008, 44, 366.
4. Ludwig, R.; Desio, G. P.; Wu, J. C. J Appl Polym Sci 1991, 42, 801.
5. Joseph, P. V.; Mathew, G.; Joseph, K.; Groeninckx, G.; Thomas, S. Compos A 2003, 34, 275.
6. Wu, C. F.; Yamagishi, T.; Nakamoto, Y.; Ishida, S.; Nitta, K.; Kubota, S. J Polym Sci Part B: Polym Phys 2000, 38, 2285.
7. Wu, C. F.; Yamagishi, T.; Nakamoto, Y.; Ishida, S.; Nitta, K.; Kubota, S. J Polym Sci Part B: Polym Phys 2000, 38, 1341.
8. Wu, C. F.; Akiyama, S. Polym J 2001, 33, 955.
9. Wu, C. F.; Akiyama, S.; Mabuchi, T.; Nitta, K. H. Polym J 2001, 33, 792.
10. Wu, C. F.; Otani, Y.; Namiki, N.; Emi, H.; Nitta, K. H.; Kubota, S. J Appl Polym Sci 2001, 82, 1788.
11. Wu, C. F. J Mater Sci Lett 2001, 20, 1389.
12. Wu, C. F.; Otani, Y.; Namiki, N.; Emi, H.; Nita, K. Polym J 2001, 33, 322.
13. Zhang, C.; Wang, P.; Ma, C. A.; Sumita, M. J Appl Polym Sci 2006, 100, 3307.
14. Wu, C. F.; Akiyama, S. Chin J Polym Sci 2002, 20, 119.
15. Li, C.; Xu, S. A.; Xiao, F. Y.; Wu, C. F. Eur Polym J 2006, 42, 2507.
16. Zhao, X. Y.; Xiang, P.; Tian, M.; Fong, H.; Jin, R.; Zhang, L. Q. Polymer 2007, 48, 6056.
17. Li, C.; Cao, D. M.; Guo, W. H.; Wu, C. F. J Macromol Sci B Phys 2008, 47, 87.
18. Ibarra, L.; Rodriguez, A.; Mora-Barrantes, I. J Appl Polym Sci 2008, 108, 2197.
19. Bandyopadhyay, S.; De, P. P.; Tripathy, D. K.; De, S. K. Polymer 1996, 37, 353.
20. Li, J.; He, Y.; Inoue, Y. J Polym Sci Part B: Polym Phys 2001, 39, 2108.
21. Wu, C. F. J Appl Polym Sci 2001, 80, 2468.
22. Rana, A. K.; Mitra, B. C.; Banerjee, A. N. J Appl Polym Sci 1999, 71, 531.
23. Idicula, M.; Malhotra, S. K.; Joseph, K.; Thomas, S. Compos Sci Technol 2005, 65, 1077.